

Electronic Supplementary Information (ESI) for:

Molecular Rotors as Reporters for Viscosity of Solutions of Collagen Like Peptides

Christopher D. McTiernan ^a, Matias Zuñiga-Bustos, ^b Roberto Rosales-Rojas, ^{b,c} Pablo Barrias, ^d May Griffith, ^{e,f}
Horacio Poblete, ^{b,g} Peter S. Sherin, ^h Ismael López Duarte, ^h Marina K. Kuimova, ^h and Emilio I. Alarcon ^{*a,i}

a. Division of Cardiac Surgery, University of Ottawa Heart Institute, 40 Ruskin Street, Ottawa, Canada.

b. Departamento de Bioinformática, Centro de Bioinformática, Simulación y Modelado (CBSM), Facultad de Ingeniería, Universidad de Talca, Campus Talca, 1 Poniente No. 1141, Casilla 721, Talca, Chile

c. Doctorado en ciencias Mención Modelado de Sistemas Químicos y Biológicos, Facultad de Ingeniería, Universidad de Talca, Campus Talca, 1 Poniente No. 1141, Casilla 721, Talca, Chile.

d. Departamento de Ciencias del Ambiente, Facultad de Química y Biología, Universidad de Santiago de Chile, Casilla 40 Correo 33, Santiago, Chile

e. Centre de Recherche Hôpital Maisonneuve-Rosemont, Montréal, QC, Canada.

f. Département d'ophtalmologie, Université de Montréal, Montréal, QC, Canada.

g. Millennium Nucleus of Ion Channels-Associated Diseases (MINICAD), Universidad de Talca, Talca, Chile.

h. Department of Chemistry, Imperial College London, South Kensington, London SW7 2AZ, UK.

i. Department of Biochemistry, Microbiology, and Immunology, Faculty of Medicine, University of Ottawa, Ottawa, Canada.

Table of Contents

S1.	Experimental Methods	S3
S2.	Supplementary Results	S5
	Figure S1. Fluorescence quantum yields and lifetimes for BDPY1 and BDPY2 measured at different viscosities	S5
	Figure S2. Fluorescence emission spectra for BDPY1 in water (480 nm excitation) measured at different temperatures	S5
	Figure S3. Changes in heat upon injection of the CLP into a 10 μ M aqueous solution of BDPY2	S6
	Figure S4. CD signal at 222 nm of 0.01% w/w TheraCol and BDPY2/ BDPY1 at different temperatures	S6
	Figure S5. BDPY1 emission spectra at various concentrations of CLP-PEG	S7
	Figure S6. Atomistic contacts between CLP and BDPY1 and BDPY2	S8
	Figure S7. Binding of BDPY1 based molecular rotor molecules to CLP	S8
	Figure S8. Contact density maps for the interaction of BDPY2 with the three-dimensional structure of CLP	S9
S3.	References	S10

S1. Experimental Methods

Chemical and reagents

Porcine type I collagen (Theracol) solution was purchased from Sewon Cellontech Co Ltd. Solutions were prepared with milli-Q water, unless otherwise noted. Acetonitrile was purchased from Sigma Aldrich. All solvents used for spectroscopic characterisation of the rotors were of spectroscopic grade. BDPY1¹ and BDPY2² and CLP-PEG³ were synthesized as previously reported.

Preparation of BODIPY stock solutions

Stock solutions of BDPY1 and BDPY2 were prepared by dissolving 1 mg/mL of the dye in acetonitrile. Aliquots of 500 μ L were then transferred to 1.5 mL Eppendorf tubes and stored in the dark at -80°C for future use.

Temperature dependence of circular dichroism (CD)

The temperature dependence of the CD signal (220 nm) of TheraCol and CLP-PEG solutions were monitored using a Model J-810 Spectropolarimeter (JASCO). Temperature was ramped between 10°C and 70°C (4.0°C /min) with CD measurements taken every 0.1°C. Solutions consisted of 10 μ M BDPY1 or BDPY2 and 0.1% w/w CLP-PEG or 0.01% w/w TheraCol. Control solutions containing only BDPY or TheraCol were prepared with the same proportion of solvents (i.e. MeCN < 1% in H₂O). Samples were prepared in a 1 mm pathlength cuvette.

Preparation and mixing of collagen-BODIPY solutions

Medical grade TheraCol porcine type I collagen as a 1% w/w solution was freeze-dried through lyophilization to give rise to a solid product which was then resuspended in Milli-Q water to give rise to a 10% w/w solution. This solution was transferred to a 10 mL disposable BD syringe and then centrifuged briefly to remove air bubbles. The 10% solution was then transferred to a 2 mL glass syringe and diluted with Milli-Q water and mixed with BDPY1 or BDPY2 to give solutions ranging from 0%-10% w/w TheraCol and 10 μ M BDPY, using a T-piece mixing system. After mixing, the solution was transferred to one of the 2 mL glass syringes, removed from the T-piece mixing system and fitted with a 18G blunt fill needle. The viscous solutions were then dispensed carefully to limit the introduction of air bubbles.

Preparation and mixing of CLP-PEG-BODIPY solutions

The CLP-PEG conjugate was prepared from a 36 amino acid peptide CG(PKG)₄(POG)₄(DOG)₄ (Amphipharm, USA) and 40K 8-Arm Polyethylene Glycol with tripentaerythritol core and terminal maleimide groups. The freeze-dried solid product was then resuspended in Milli-Q water to give rise to a 10% w/w solution in a 10 mL disposable BD syringe, which was heated to 50°C and then centrifuged briefly to remove air bubbles. The 10% w/w solution was then transferred to a 2 mL glass syringe and diluted with Milli-Q water and mixed with BDPY1 or BDPY2 to give solutions ranging from 0%-10% w/w CLP-PEG and 10 μ M BDPY, using a T-piece mixing system. After mixing, the solution was transferred to one of the 2 mL glass syringes, removed from the T-piece mixing system and fitted with a 18G blunt fill needle. The viscous solutions were then dispensed carefully to limit the introduction of air bubbles.

Viscosity measurements

Viscosity measurements were carried out on the solutions prepared above using a Brookfield R/S plus rheometer (Brookfield). A C25-1 conical spindle was used to compress the material onto a temperature-controlled pedestal. Measurements were recorded using controlled shear rate of 6 s⁻¹ over 60 s.

Steady-state absorption, fluorescence, and fluorescence anisotropy measurements

Absorption spectra were recorded using a SpectraMax M2e (Molecular Devices) microplate/cuvette reader. Fluorescence and fluorescence anisotropy measurements were performed on a LS55 Spectrofluorimeter (Perkin Elmer). All measurements were recorded using a 5 mm quartz cuvette unless otherwise stated.

Fluorescence intensity and lifetime calibration measurements

Viscosity calibrations were carried out with BDPY 1 and BDPY2 in dry glycerol of highest purity (Sigma Aldrich) at different temperatures. Samples were prepared by addition of 0.2 μ L of BDPY stock solutions (3mM, DMSO) to 2 mL of

glycerol. The resulting samples with absorption below 0.1 at the maximum were placed in 1 cm quartz cuvettes with screw caps. Viscosity of glycerol at different temperatures were taken from ⁴.

Fluorescence intensity calibration was carried out by recording of fluorescence spectra with FluoroMax-4 spectrophotometer (Jobin-Yvon, Horiba) equipped with the automated Peltier-based thermostat F3004 (Jobin-Yvon, Horiba). Measurements were performed in a temperature range of 10 – 80°C. Samples were excited at 470 nm and fluorescence spectra recorded in the range 480-650 nm and corrected for the wavelength sensitivity of detector. Fluorescence Quantum Yields (QYs) were determined relatively to fluorescein in 0.01 M NaOH (0.93)^{5,6}. QY values were corrected for the refractive indexes of glycerol and water used for samples and standard, respectively; the temperature influence on the glycerol refractive index was neglected.

Lifetime calibration was performed for BDPY-2 and the corresponding data for BDPY-1 was taken from⁷. Time-resolved kinetics of fluorescence decays were recorded with home-built Time-Correlated Single Photon Counting (TCSPC) setup consisted of a BDL-488 SMN ps diode laser (Becker & Hickl) operating at 20 MHz frequency, a SPC-830 photon counting card (Becker & Hickl), a DCC-100 detector control module (Becker & Hickl), a PMC-100-1 photomultiplier tube (Hamamatsu), Omni-λ grating monochromator (LOT-Quantum Design), qpod cuvette holder and TC125 Peltier thermostat (Quantum Northwest). Measurements were performed in a temperature range of 5 – 100°C, the temperature inside the solution was additionally verified by a thermocouple 2006T (Digitron). The excitation was performed at 488 nm and fluorescence kinetics were recorded at 510 nm after passing through a 500 nm long-pass filter. The number of photons at the peak of all traces was 20000 counts. The time window for acquiring fluorescence decays was 50 ns with 4096-time bins. The instrument response function (IRF) was recorded using a scattering Ludox® solution. Fluorescence lifetimes were obtained from kinetics fitting using SPCImage v.8.3 (Becker & Hickl) software and the monoexponential incomplete decay numerically convolved with IRF. The goodness of fits was controlled by visual agreement between experimental and fitted kinetics and confirmed by the value of χ^2 parameter in the range below 1.2.

Isothermal titration calorimetry (ITC)

Changes in heat from BDPY2 to CLP were analyzed using a VP-ITC MicroCalorimeter Malvern Isothermal titration calorimeter system. Briefly, 2 mL of a freshly prepared BDPY2 10 μ M solution and 2 mL ultrapure water were degassed for 15 min and loaded into the ITC sample cell and reference cell, respectively. The temperature was calibrated to 25 °C and the injection syringe was loaded with 300 μ L of the peptide (1.0 mM). Parameters were set as: 25 injections, 1.5 μ L per injection, 5 s injection time, and 300 s injection spacing. Each run was analyzed using Microcal Origin and data extracted for plotting in Kaleida Graph 5.0.

Computational details

The molecular structures of BDPY1 and BDPY2 were constructed and optimized using Chimera software.⁸ The parameters of BODIPY-core were adapted according to the model of Song et al.⁹ The attached hydrocarbon tail of BDP1 and BDP2 were positioned in a meso conformation to the core; additionally, it was parametrized using Paramchem¹⁰ server through the CHARMM General Force Field (CGenFF)^{10, 11}. Also, our group previously developed the model of CLP1 structure using the CHARMM36 parameters.^{12, 13} In each simulation, a single molecule of BDIPY was randomly positioned at 10 Å of the peptide and solvated with an explicit periodic TIP3P water box of 50x54x160 Å³, and neutralized using a 0.15 nM of Na⁺ and Cl⁻ counterions to ensure a neutral charge of the system. All systems were minimized during 25000 steps, following by equilibrium and production simulations of 20 ns and 200 ns, respectively, setting the temperature to 10°, 30°, and 70°C degrees. Hydrogen covalent rigid bond restrictions (SHAKE)¹⁴, particle-mesh Ewald electrostatic¹⁵ with 9 Å of cutoff, Langevin thermostat and piston barostat¹⁶, and 4fs of time step were set into the simulations.¹⁷ All molecular dynamics simulations were performed using the NAMD 2.13 package¹⁸ and subsequently visualized and analyzed on VMD software.

S2. Supplementary results

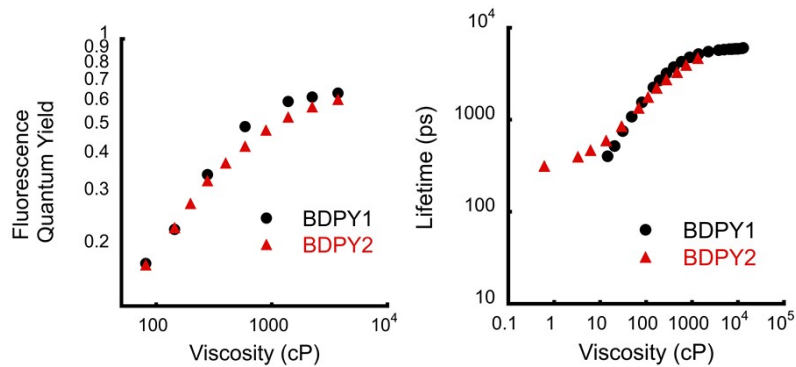


Figure S1. Left: Fluorescence quantum yields (QY) for BDPY1 and BDPY2 measured at different viscosities in glycerol solutions at different temperatures. Right: Fluorescence lifetime for BDPY1 and BDPY2 measured at different viscosities. It is clear to see that both QY and lifetime curves show excellent overlap, which could be expected from their very similar molecular structures, Scheme 1 of the main text. For BDPY2, we infer that the differences in fluorescence intensities seen upon interaction with CPL are, indeed, due to different interactions between these rotors with CPL, rather than differences in calibration vs viscosity. We hypothesise that additional charges on BDPY2 make it more hydrophilic and aid interactions with CPL.

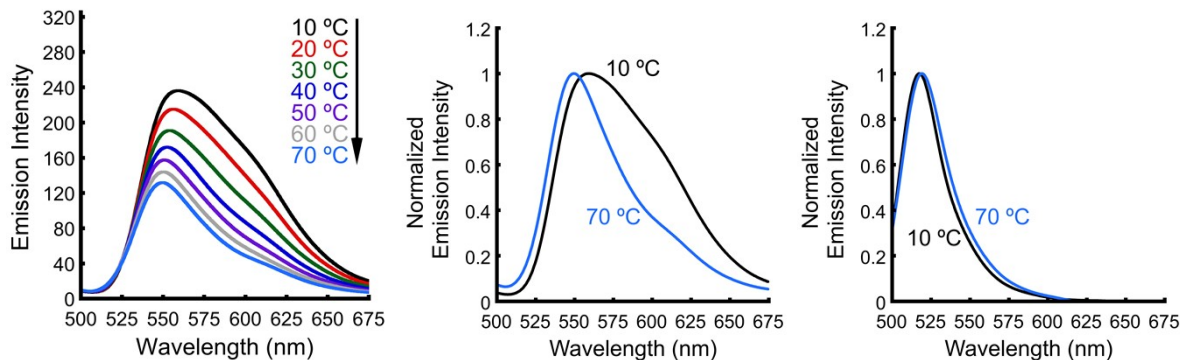


Figure S2. (Right) Fluorescence emission spectra for BDPY1 in water (480 nm excitation) measured at different temperatures. Normalised spectra at 10 and 70°C are shown in **Centre** for BDPY1 and in **Left** for BDPY2. While the normalised spectra coincide for BDPY2, the spectra for BDPY1 show significant broadening at lower temperature. The shape of these emission spectra may indicate the formation of aggregates in solution whose population is reduced as temperature increases. The possible aggregation is further confirmed by the data shown in Figure S5.

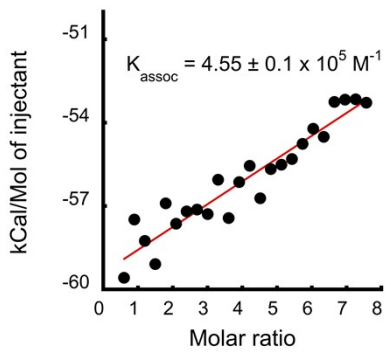


Figure S3. Changes in heat upon injection of the CLP into a 10 μM aqueous solution of BDPY2. Changes in heat were used to calculate association constant for the binding process (see experimental, $R \approx 0.95$).

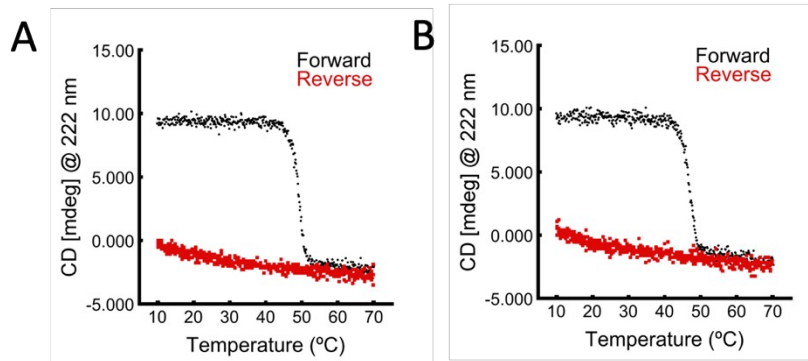


Figure S4. (A) CD signal at 222 nm of 0.01% w/w TheraCol, and (B) CD signal at 222 nm of a mixture of 10 μM BDPY2 and 0.01% w/w TheraCol measured as a function of temperature. Forward scan (10 °C – 70 °C) Reverse scan (70 °C – 10 °C).

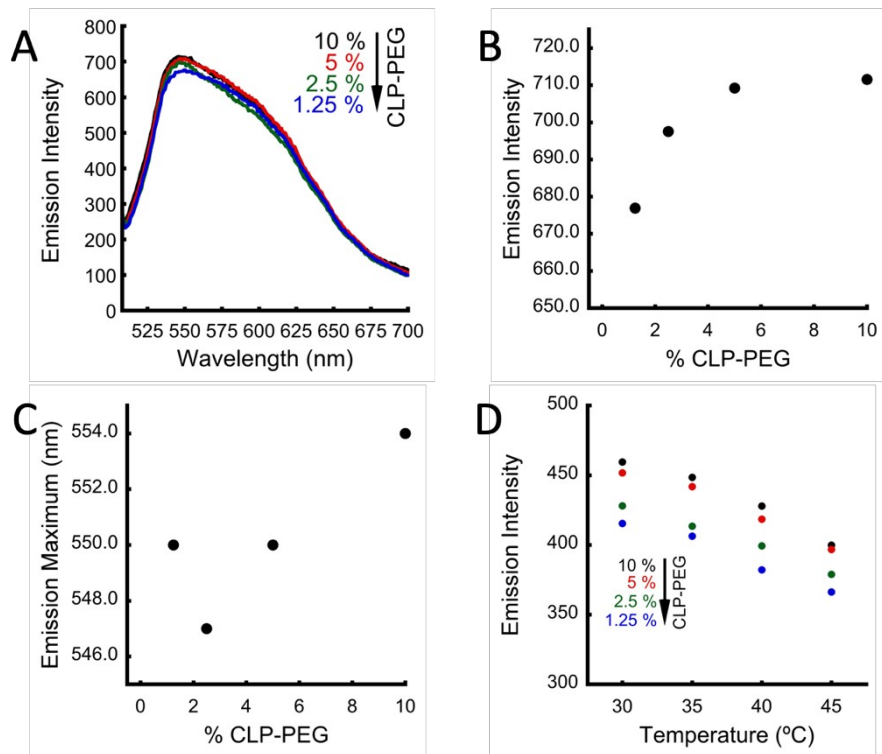


Figure S5. BDPY1 emission spectra at various concentrations of CLP-PEG. (A) (B) Fluorescence spectra of 10 μ M BDPY1 in increasing concentrations of CLP-PEG. (B) Changes in fluorescence intensity as a function of increasing CLP-PEG concentration. (C) Changes in emission maximum as a function of increasing CLP-PEG concentration (D) Emission intensity at maximum of BDPY1 in various concentrations of CLP-PEG at temperatures between 30 °C and 45 °C.

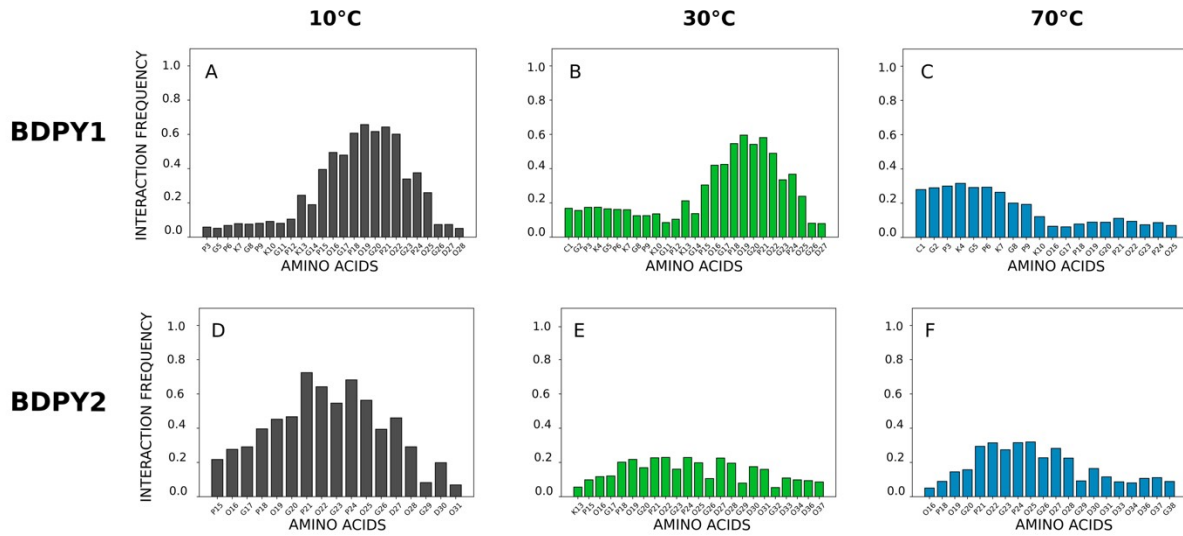


Figure S6. Atomistic contacts between CLP and BDPY1 and BDPY2. (A) Contact frequency between CLP and BDPY1 at 10 °C, (B) 30 °C and (C) 70 °C. (D) Contact frequency between CLP and BDPY2 at 10 °C, (E) 30 °C and (F) 70 °C.

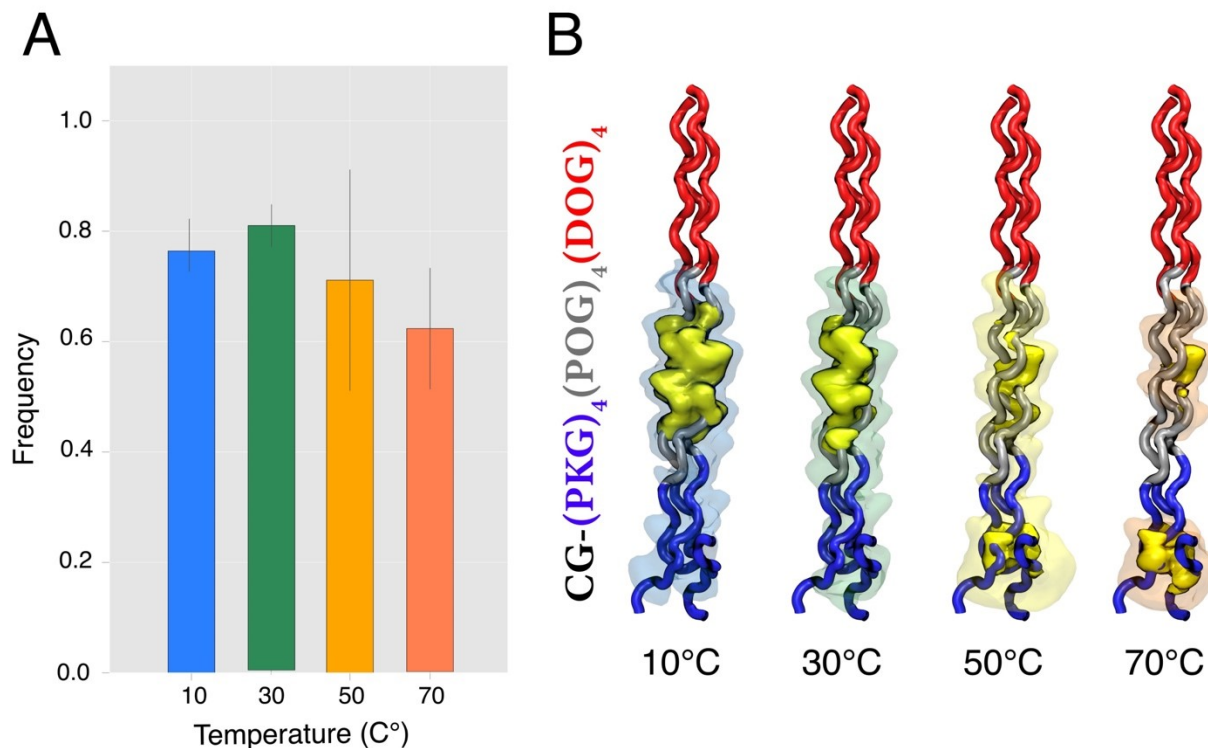


Figure S7. Binding of BDPY1 based molecular rotor molecules to CLP. (A) Contact frequency ratio between BDPY1 to CLP over a 500ns simulation. (B) Three-dimensional contact map of BDPY1 with CLP at different temperatures. Yellow surfaces represent where BDPY1 remains for greater than 40% of the simulation time, while transparent surfaces (Blue, green, orange, or red) represent where BDPY1 stays greater than 60% of the simulation time.

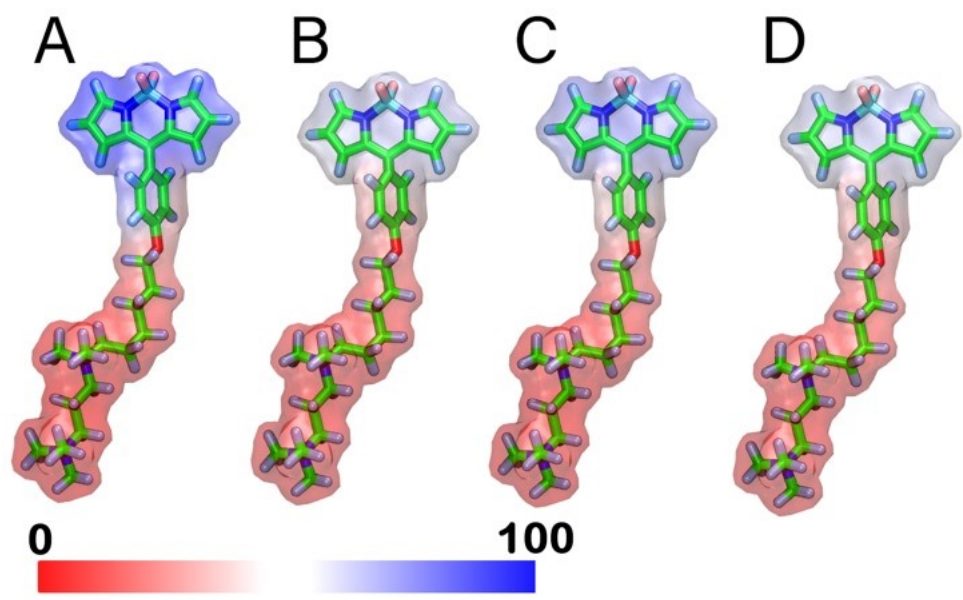


Figure S8. Contact density maps for the interaction of BDPY2 with the three-dimensional structure of CLP. Simulations run at 10 °C (A), 30 °C (B), 50 °C (C), and 70 °C (D) degrees. Colouring represents contact density from 0% (red) to 100% (blue).

S3. References

1. J. A. Levitt, M. K. Kuimova, G. Yahioglu, P.-H. Chung, K. Suhling and D. Phillips, *J Phys Chem C*, 2009, **113**, 11634-11642.
2. I. López-Duarte, T. T. Vu, M. A. Izquierdo, J. A. Bull and M. K. Kuimova, *Chem Comm*, 2014, **50**, 5282-5284.
3. M. M. Islam, R. Ravichandran, D. Olsen, M. K. Ljunggren, P. Fagerholm, C. J. Lee, M. Griffith and J. Phopase, *RSC Adv*, 2016, **6**, 55745-55749.
4. *J Am Pharm Association*, 1953, **42**, 326-326.
5. G. Weber and F. W. J. Teale, *Trans Faraday Soc*, 1957, **53**, 646-655.
6. D. M. Hercules and H. Frankel, *Science (New York, N.Y.)*, 1960, **131**, 1611-1612.
7. Y. Wu, M. Štefl, A. Olzyńska, M. Hof, G. Yahioglu, P. Yip, D. R. Casey, O. Ces, J. Humpolíčková and M. K. Kuimova, *Phys Chem Chem Phys*, 2013, **15**, 14986-14993.
8. T. D. Goddard, C. C. Huang and T. E. Ferrin, *Structure*, 2005, **13**, 473-482.
9. K. C. Song, P. W. Livanec, J. B. Klauda, K. Kuczera, R. C. Dunn and W. Im, *J Phys Chem B*, 2011, **115**, 6157-6165.
10. K. Vanommeslaeghe, E. Hatcher, C. Acharya, S. Kundu, S. Zhong, J. Shim, E. Darian, O. Guvench, P. Lopes, I. Vorobyov and A. D. MacKerell Jr, *J Comp Chem*, 2010, **31**, 671-690.
11. W. Yu, X. He, K. Vanommeslaeghe and A. D. MacKerell Jr, *J Comp Chem*, 2012, **33**, 2451-2468.
12. E. I. Alarcon, H. Poblete, H. Roh, J.-F. Couture, J. Comer and I. E. Kochevar, *ACS Omega*, 2017, **2**, 6646-6657.
13. C. D. McTiernan, D. C. Cortes, C. Lazurko, S. Amrani, R. Rosales-Rojas, M. Zuñiga-Bustos, V. Sedlakova, H. Poblete, K. Stampeloskie, E. J. Suuronen and E. I. Alarcon, *ACS Appl Mat Interfaces*, 2019, **11**, 45007-45015.
14. S. Miyamoto and P. A. Kollman, *J Comp Chem*, 1992, **13**, 952-962.
15. T. Darden, D. York and L. Pedersen, *J Chem Physics*, 1993, **98**, 10089-10092.
16. S. E. Feller, Y. Zhang, R. W. Pastor and B. R. Brooks, *J Chem Physics*, 1995, **103**, 4613-4621.
17. C. W. Hopkins, S. Le Grand, R. C. Walker and A. E. Roitberg, *J Chem Theory Comp*, 2015, **11**, 1864-1874.
18. J. C. Phillips, R. Braun, W. Wang, J. Gumbart, E. Tajkhorshid, E. Villa, C. Chipot, R. D. Skeel, L. Kalé and K. Schulten, *J Comp Chem*, 2005, **26**, 1781-1802.